Progress Report No. 3

MECHANISM OF THE PHOTOVOLTAIC EFFECT IN II-VI COMPOUNDS

National Aeronautics and Space Administration
Lewis Research Center
Cleveland, Ohio

April 1, 1968 - September 30, 1968

School of Engineering
Department of Materials Science
Stanford University
Stanford, California

Grant NGR-05-020-214

Principal Investigator

Richard H. Bube, Professor

Report Prepared By:

R.H.Bube
W.D.Gill
P.F.Lindquist

SU-DMS-69-R-2

Department of MATERIALS SCIENCE
STANFORD UNIVERSITY

Progress Report No. 3

MECHANISM OF THE PHOTOVOLTAIC EFFECT IN II-VI COMPOUNDS

National Aeronautics and Space Administration
Lewis Research Center
Cleveland, Ohio

April 1, 1968 - September 30, 1968

School of Engineering
Department of Materials Science
Stanford University
Stanford, California

Grant NGR-05-020-214

Report No. SU-DMS-69-R-2

Principal Investigator

Richard H. Bube, Professor

Report Prepared By:

R.H.Bube
W.D.Gill
P.F.Lindquist

CONTENTS

Progress Report No. 3 April 1 - September 30, 1968

SUMMARY

Phenomena involved in the observation of large current gains upon photoexcitation in the presence of a small reverse bias were examined in considerably greater detail. When a variety of related experimental observations are taken into account - the apparent decrease in the barrier height under illumination, the low open-circuit voltage obtainable, and the effect of heat treatment on cell efficiency - it appears that a mechanism is present which is responsible for (1) current leakage paths under forward bias in dark or light, (2) removal of these leakage paths under reverse bias in the dark, and (3) activation of these leakage paths under reverse bias by photoexcitation to produce the large gains measured. The phenomena presented in this way are very similar to that expected for some kind of field-modulated depletion process, as in a photo-FET. Whether this similarity is more than apparent is the subject of continued investigation. No model constructed to date is completely satisfactory.

Depletion layer widths were investigated using the light microprobe, electron mirror microscope photographs, effects of chemical etching, and improved capacitance vs. voltage measurements. Large apparent depletion widths measured regularly with the microprobe, EMM, and etching must be associated with the effects of surface states. A barrier height of 1.1 eV was obtained from a plot of $1/C^2$ vs. V for a cell giving a straight line on such a plot, and excellent agreement was found between the (N_D-N_A) obtained from this plot and bulk resistivity data. The light I-V characteristic remains below the dark characteristic over the entire measured range, indicating that leakage paths are not important in this sample. Several other samples, whose capacitance data indicate close to ideal Schottky barrier behavior, also indicate barrier heights of about 1 eV.

Spectral response data obtained with the microprobe indicate considerably more red response on the CdS side of the junction than on the Cu_2S side.

I. PHOTOCURRENT GAIN WITH APPLIED BIAS VOLTAGE

A. Experimental

Observations of a large current-gain effect on the application of small reverse bias voltage were described in the last report.[1] Since that time the effect has been observed in a large number of single crystal CdS samples as well as on the evaporated CdS cells produced by Clevite Corporation.

Gain, which is here defined as the observation of more photoinduced current than incident photon flux, has been seen in the following situations: (1) Shining a small spot of highly absorbed blue light on the CdS side of a bevelled Cu_2S-CdS heterojunction. Bevel angles of + and -5° have been used. Positive angles are those for which a wedge of CdS is formed at the bevelled surface, and negative angles are those for which a wedge of Cu_2S is formed. (2) Shining a small spot of blue light on the Cu_2S surface of a thin Cu_2S layer heterojunction formed on a single crystal of CdS. (3) Shining the spot of blue light on the Cu_2S side of a Clevite evaporated CdS photocell.

Observations of a large number of samples under a variety of conditions may be summarized as follows:

(1) Large gain (up to 300) is seen on all bevelled samples with highly absorbed light incident on the active region of the junction at the surface. (see Fig. 1 and 2).

(2) Smaller gain ($\approx$2) is seen when blue light is incident on the frontwall side of very thin Cu_2S layers, on both single crystals CdS and on the evaporated CdS (Clevite cell) heterojunctions.

(3) No gain is observed in any geometry with photons of lower energy than the bandgap of CdS.

(4) For photons with energy greater than the bandgap of CdS on bevelled junctions, the gain is always greatest at the edge of the active region farthest away from the metallurgical interface (Fig. 1).

(5) There is no reverse bias threshold for onset of the observed gain. (Fig. 2).

(6) Saturation of the gain occurs at reverse bias of about 2 to 5 volts. Saturation occurs earlierwith lower light intensity.

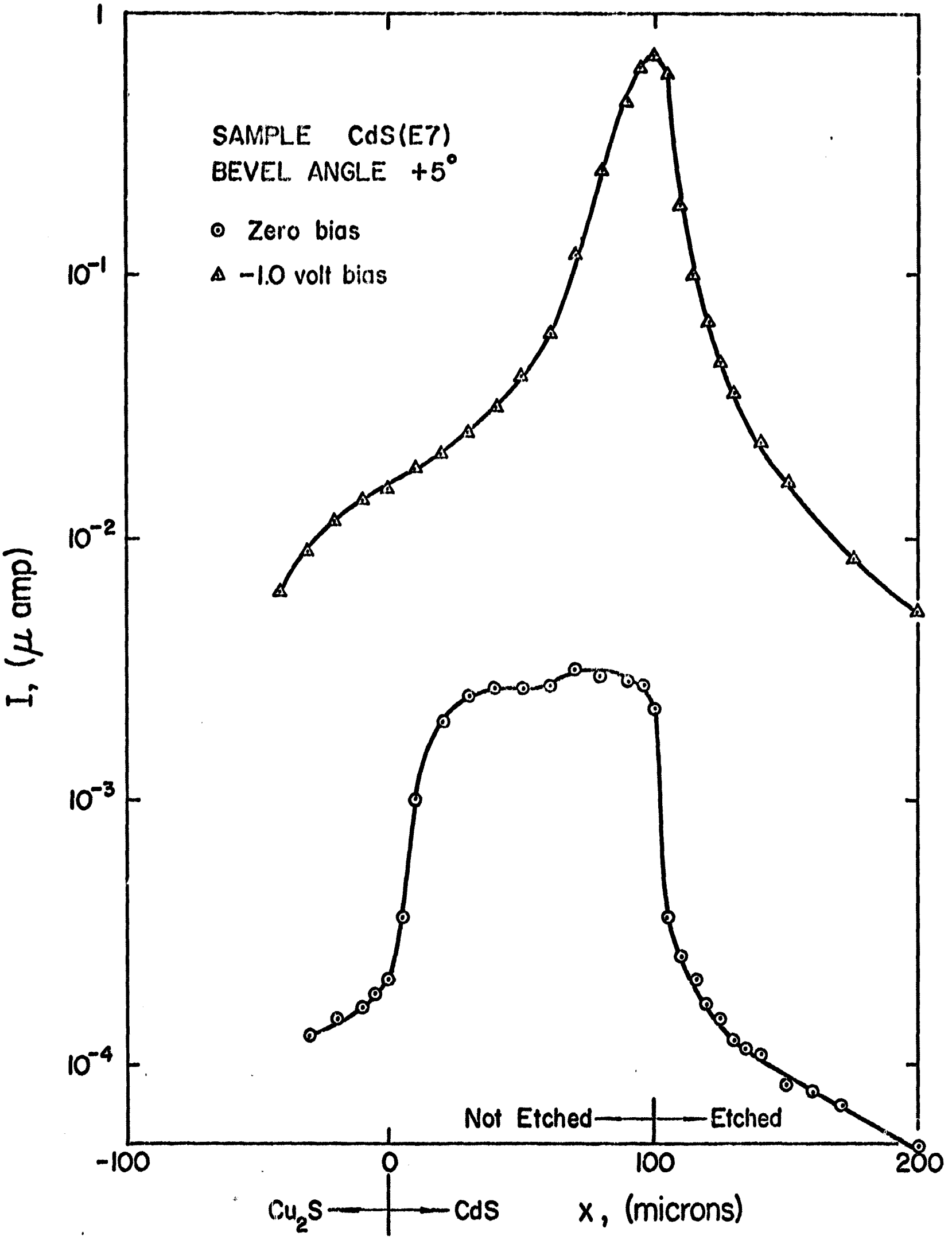

Fig. 1. Photocurrent versus light spot position for sample CdS(E7) with and without reverse bias. For the +5° bevel angle the measured distances should be multiplied by 0.087 to get the perpendicular distance to the junction. Etched/not etched regions refer to results of etching with $H_2SO_4 + KMnO_4$ (see Fig. 8).

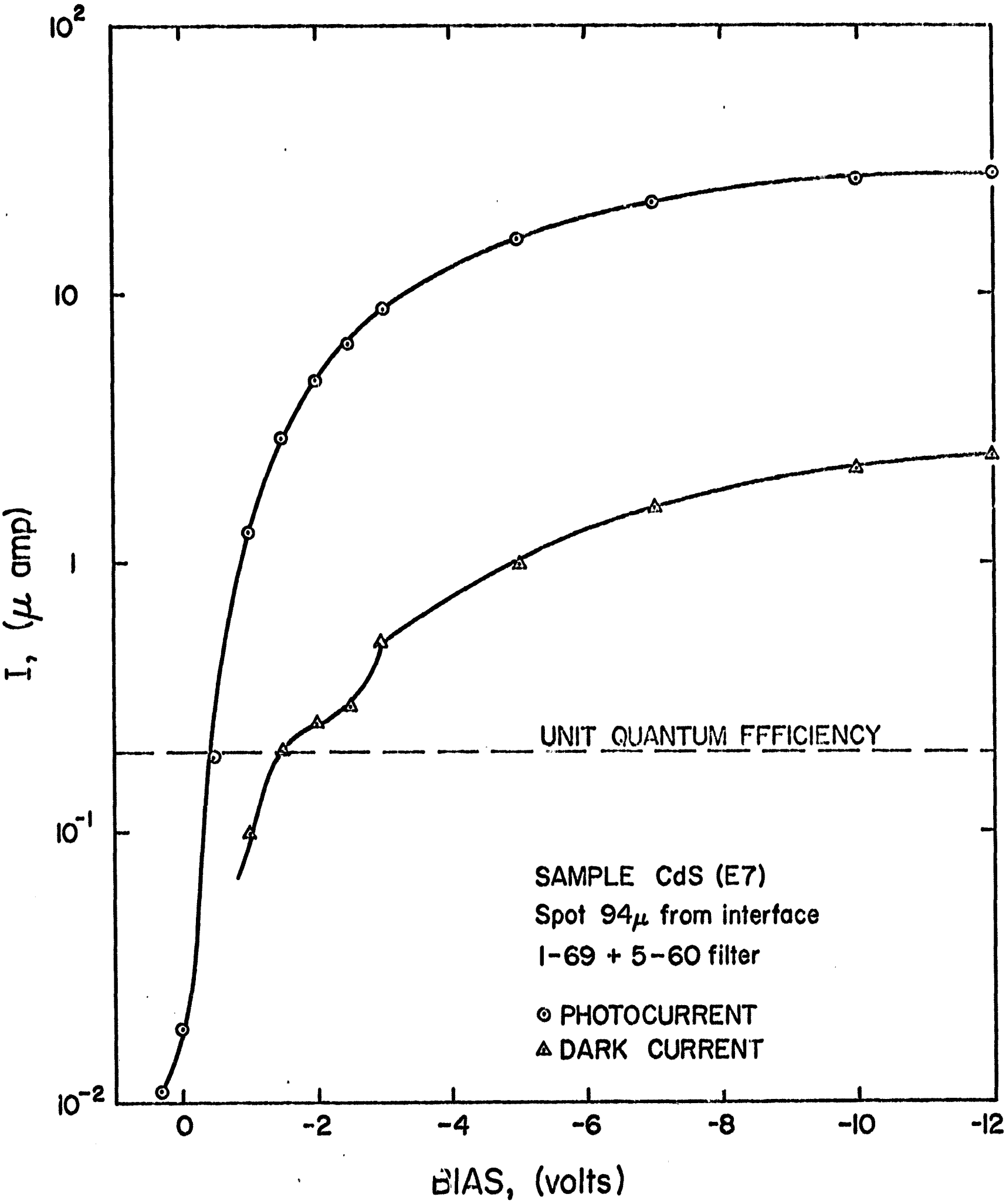

Fig. 2. Photocurrent and dark current versus reverse bias voltage for sample CdS(E7). The distance from the light spot to the junction was 94(.087) = 8.2 microns. Unit quantum efficiency line corresponds to the total light flux measured with a calibrated silicon photodiode.

(7) Short-circuit current and gain vary greatly over 5 to 10 μ intervals parallel to the junction.

(8) Gain decreases after heat treatment.

(9) Gain with forward bias is seen in some samples. Reproducibility is poor, but gain is maximum at about 0.6 eV and cuts off completely at about 1 volt.

(10) The photocurrent is much larger than the dark current in some samples having particularly good reverse current characteristics (Fig. 2).

B. Discussion

Considering the observations listed above we can make the following conclusions about the mechanism giving rise to the large photocurrent gain.

(1) High gain is related to hole transit time which (neglecting trapping effects) should be about 10 times the electron transit time. This conclusion is based on observation (4) that the greatest gain is achieved at the farthest region from the junction (Fig. 1). Therefore, the mechanism depends on the time that injected carriers spend in the active region.

(2) The large observed gains cannot be caused by avalanche breakdown or impact ionization. This conclusion comes from considerations (5) and (6). Avalanche breakdown requires a threshold energy of at least 3/2 E_g which for CdS would require a reverse bias of at least 3.5 volts. Also no saturation should be seen with an avalanche process. At room temperature similar energy considerations hold for impact ionization since only deep impurities could be affected

(3) Modulation of the dc dark current, considered likely in the last report,[1] does not seem to be an adequate mechanism in view of observation (10) where light-induced-current up to 20 times I_{dark} has been observed (Fig. 2).

(4) Normal photoconductive gain alone can be rejected as a possible mechanism since no additional sources for carrier injection are available. The reverse current is made up of a diffusion current and a generation current neither of which provide a carrier source for multiplication of injected charge.

C. Leakage Model

In view of these conclusions some other mechanism was sought, which could explain the observed results of the gain phenomena, and still be consistent with other measurements of I-V characteristics and capacitance measurements on these samples. The principal requirements of such a mechanism appear to be its ability to account for (1) current leakage phenomena under forward bias in dark or light, (2) absence of such leakage under reverse bias in the dark, and (3) re-introduction of this leakage under reverse bias with photoexcitation to produce the large measured gains.

The fact that large apparent gains are seen in all samples, both polycrystalline CdS and single crystal CdS, suggests a simple mechanism is operative. The possibility of light-sensitive leakage together with the concept of photoconductive gain is consistent. Leakage paths are certainly present as can be seen from the high values of reverse-bias dark current and the low reverse breakdown characteristics of the cells. The most probable locations for such leakage paths are internal or external surfaces, where the high density of surface states can give rise to high rates of generation and recombination. The phenomena observed are very similar to that expected for some kind of field-modulated depletion process, as in a photo-FET. Whether this similarity is more than apparent is the subject of continued investigation. No model constructed to date is completely satisfactory.

D. Effect on Light and Dark I-V Characteristics

The effect of a light-sensitive leakage path on the light and dark I-V characteristics is illustrated in Figures 3 and 4. For any arbitary form of the leakage current, which increases in magnitude over its dark value, we see that $V_B > V_B' > V_B''$, where these voltages are obtained from the extrapolated linear portions of the forward characteristics for, respectively, the ideal diode, the diode with dark leakage current, and the diode with light leakage current. The increased leakage in the light gives rise to the anomalous forward characteristics observed in most samples.

E. Effects of Leakage Model on Photocell Behavior

A generalized leakage model might be expected to have the following effects on the operation of these heterojunctions as photovoltaic cells.

(1) Leakage paths will have no effect on I_{sc} as long as the external

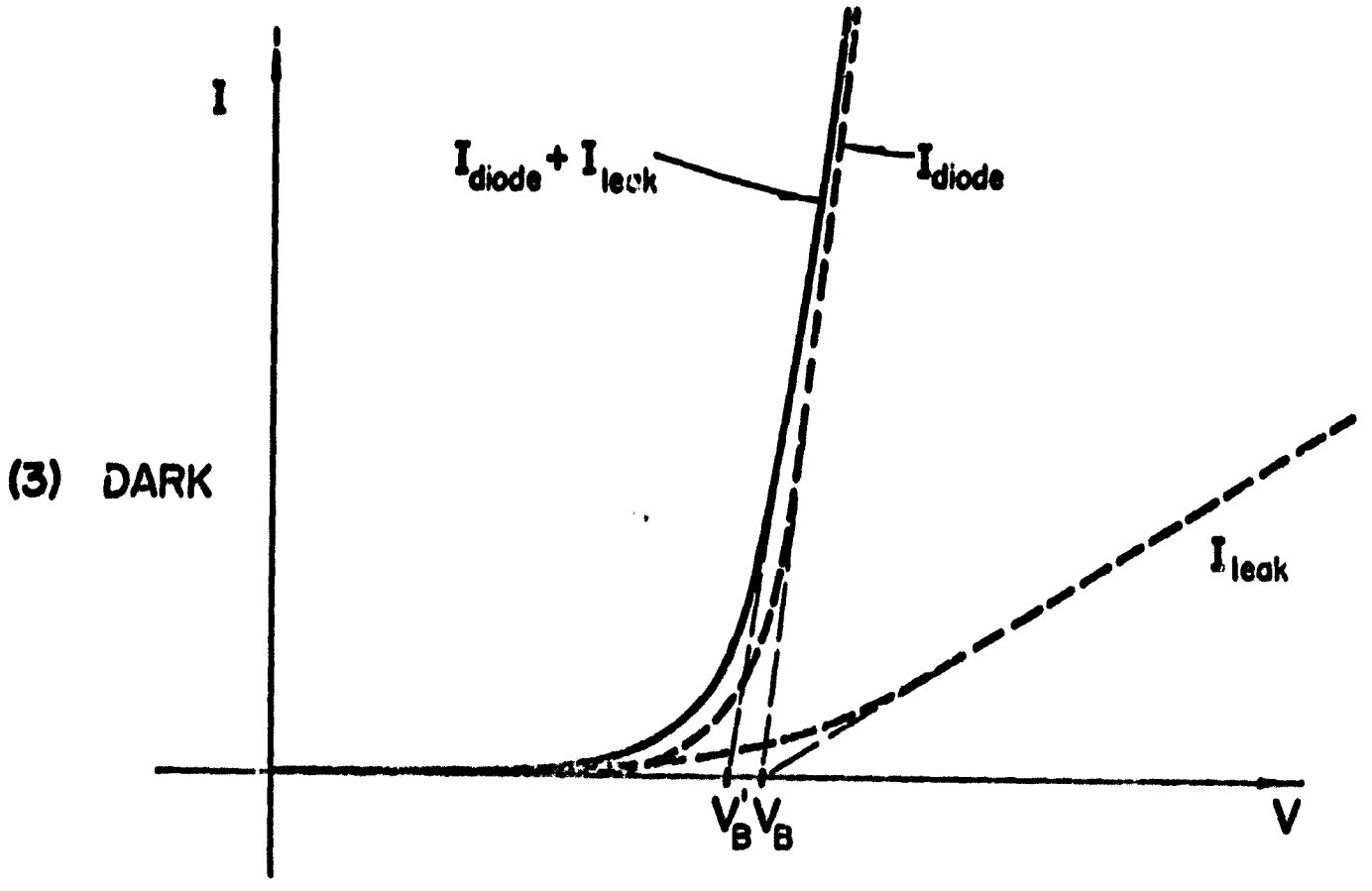

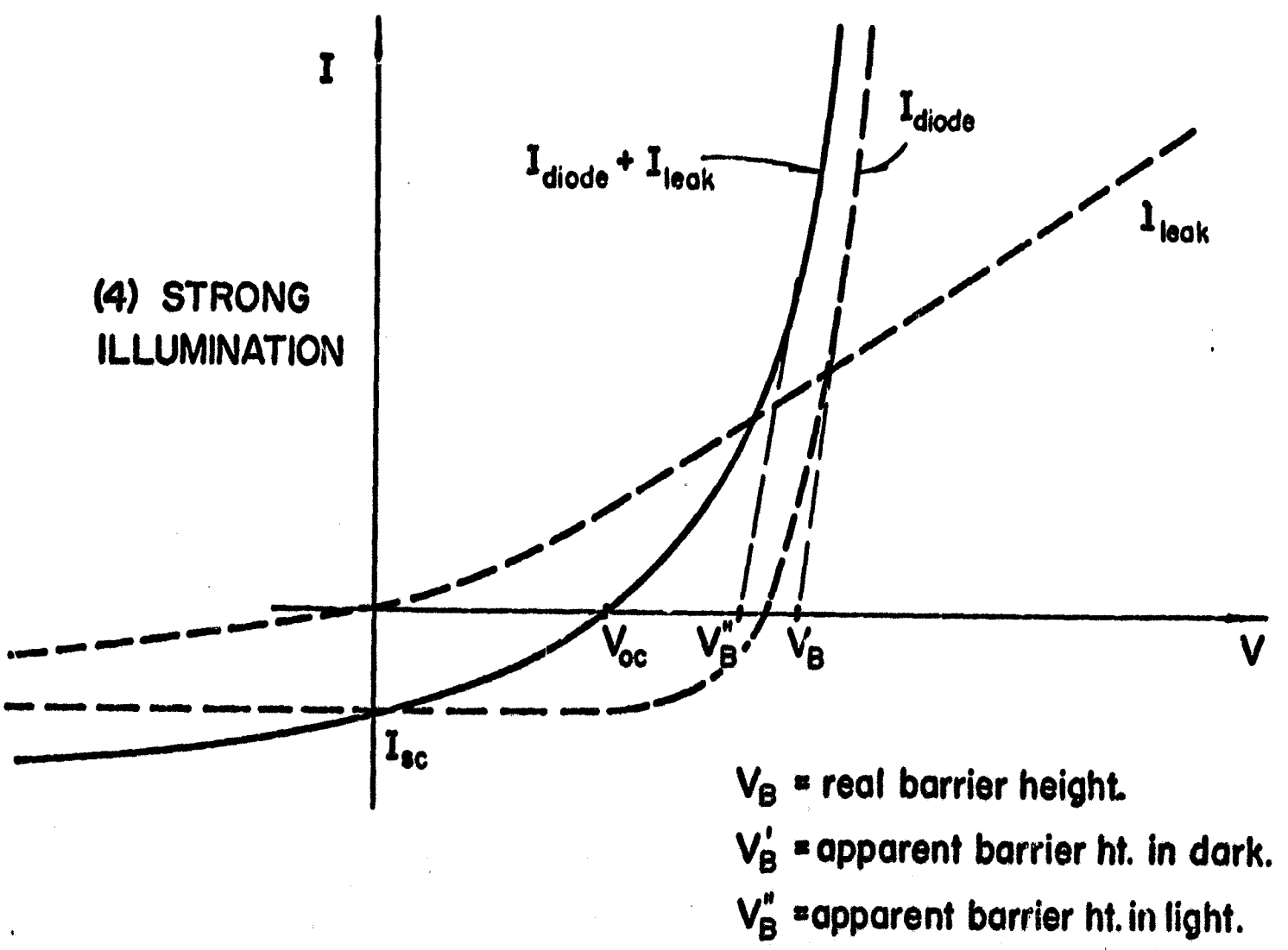

Fig. 3. Form of the dark I-V characteristic for a junction with leakage.

Fig. 4. Form of the light I-V characteristic for a junction with leakage.

load resistance used to make the measurement is small.

(2) Referring to Figs. 3 and 4, we see that V_B' will be less than V_B, and that V_B'' will be less than V_B'. These three voltages are obtained by extrapolating the linear parts of the forward characteristics to cut the voltage axis. The voltage obtained in this manner are often used as a rough measure of the built-in voltage or barrier height of the cell. The presence of leakage paths would lead to an underestimate of the barrier height and would result in an apparent decrease of the barrier under illumination. The measurement of saturated V_{oc} at low temperatures would be subject to the same difficulties.

(3) Forward current under illumination would be expected to be greater than the dark current.

(4) Largest V_{oc} should be measureable using photons with energy less than the bandgap of CdS. Additional strong bandgap illumination of the junction may result in a decrease in V_{oc} if large leakage paths exist. This effect has been observed.

(5) Short heat treatment should improve cell performance by decreasing the influence of leakage paths. However, the forward current under strong illumination might still be greater than the dark forward current, since the leakage paths are light-sensitive.

(6) Cell efficiency should be improved by short heat treatment. Higher leakage resistance will increase V_{oc}, and even if decreased I_{sc} should result, the increased leakage resistance out to higher forward voltages improves the filling factor.

F. Summary of Leakage Model

In the preceding sections experimental data have been presented which indicate the importance of a light-sensitive leakage mechanism in the operation of the Cu_2S-CdS heterojunction. Although not yet specifically defined, the model

provides a reasonable mechanism for the large photocurrent gain which has been observed at small reverse bias. In addition this model predicts many of the results actually observed in these heterojunctions, such as the apparent decrease in the barrier height under illumination, the low V_{oc} obtainable with these cells, and the effect of heat treatment on cell efficiency.

G. Observation of Multiplication Effect for Wavelengths Longer than CdS Band Edge

A single crystal (#4-92R) was prepared in the usual manner by dipping in a CuCl solution for one hour at 90°C. The Cu_2S layer was formed on the "A" face of the crystal, which was etched in H_2SO_4 + $KMnO_4$ for 15 seconds before dipping. The resistivity of the CdS was 19.0 ohm-cm. This cell had a back-wall spectral response curve which was modified significantly by superimposing a DC reverse bias of 3 volts. This is illustrated in Fig. 5. Note that the short-circuit current is increased for wavelengths less than 800 mμ, but is suppressed at longer wavelengths. The curves have been normalized to a constant photon flux of 5.8×10^{14} $cm^{-2}sec^{-1}$. The discontinuity at 700 m μ (upper point: 2-64 filter out; lower point: filter in), which remains after correcting for equal intensity, may indicate a non-linear dependence of the short-circuit current on light intensity when the cell is under reverse bias.

In terms of power output, this cell was relatively very poor, having a linear light I-V characteristic with V_{oc} = 40 mv and I_{sc} = 12 μa in white tungsten light of 280 mw/cm^2 integrated power. The measurement of spectral response with DC bias was recently repeated on a relatively very good cell, and it was found that the effect of the reverse bias was considerably smaller, increasing the short-circuit current about 10-50% over the entire response range. Table I gives the computed quantum yield of the cell #4-92R as a function of the applied DC bias, at a wavelength of 540 m μ. The values of quantum yield may be in error by a constant factor because of an uncertainty in the cell area.

TABLE I. Quantum Yield Vs. DC Reverse Bias for Cell #4-92R at 540 m μ

V_{DC}, Volts	Electrons/Photon
0	3.66×10^{-2}
-1	6.18×10^{-2}
-2	11.45×10^{-2}
-3	18.6×10^{-2}

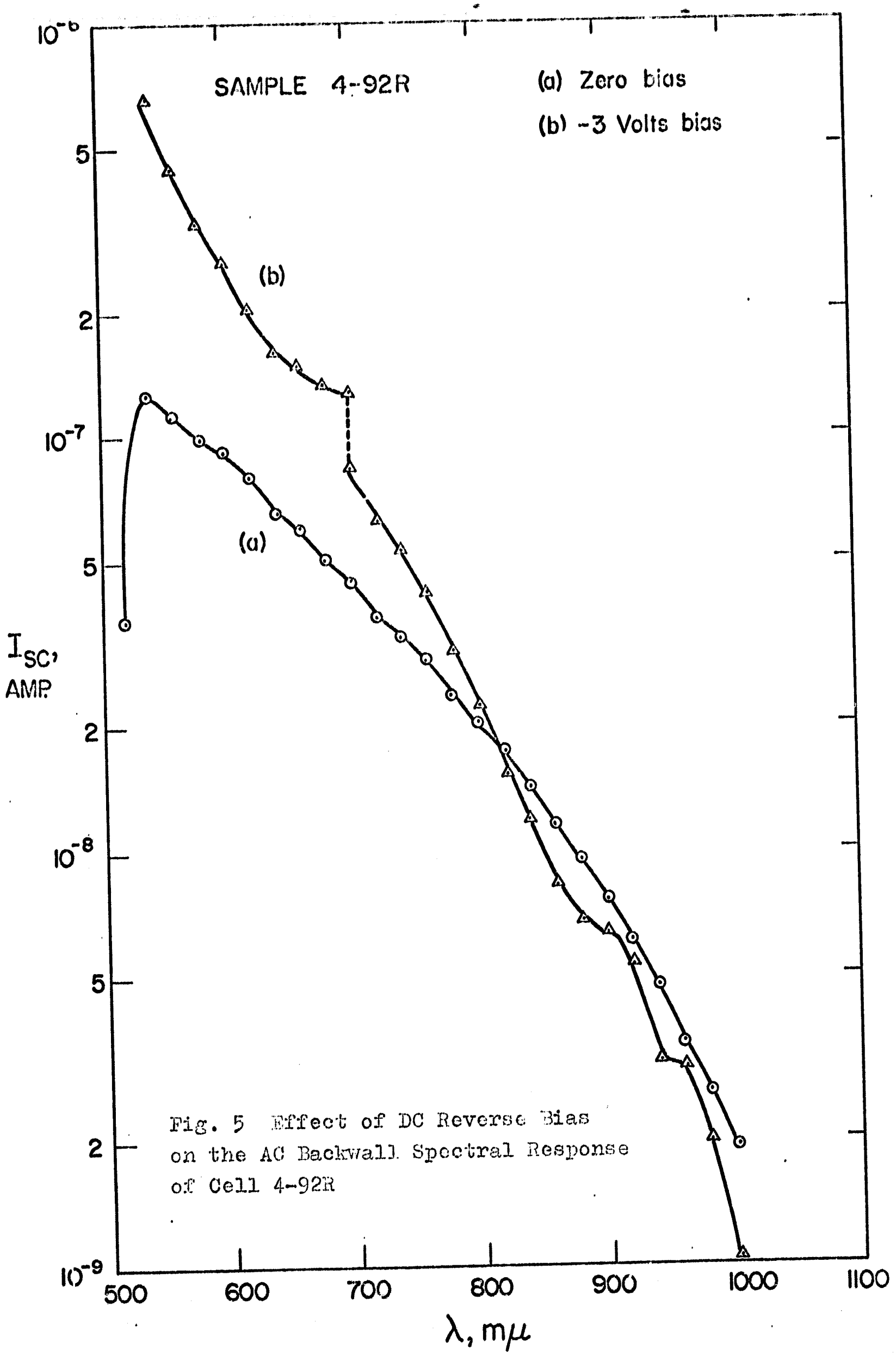

Fig. 5 Effect of DC Reverse Bias on the AC Backwall Spectral Response of Cell 4-92R

The capacitance of this cell at zero bias (1 MHz, 540 m μ) was 172 pf, which corresponds to a depletion layer width of about 3 microns. The capacitance with voltage applied was not measured.

II. DEPLETION LAYER WIDTHS

A. Light Microprobe Measurements

Measurement of the depletion layer thickness provides a direct measurement of the impurity profile and its variation with heat treatment in the vicinity of the junction. Early difficulties in obtaining meaningful capacitance versus reverse bias data led us to develop the light microprobe in an attempt to measure directly the depletion layer width and diffusion lengths. The light microprobe measurements are of necessity surface measurements and hence very sensitive to surface conditions. Examples of the wide depletion layers measured with the light probe are seen in Figures 1 and 10. Better understanding of the limitations of our capacitance bridge now allows us to make reliable capacitance measurements by adjusting sample geometry to stay within the conductance capabilities of the instrument. These measurements show that before heat treatment the junctions can be regarded as very nearly ideal Schottky barriers. The depletion widths obtained capacitively represent the bulk value and are found in general to be an order of magnitude smaller than those measured with the travelling light spot.

B. Electron Mirror Microscope Photographs

Two other surface measurements of the depletion width have been made, both agreeing well with the light probe results. Photographs of the field at a reverse biased junction were obtained using an electron mirror microscope.[2] A very low energy electron beam is deflected by fringe fields immediately outside the surface of the sample and forms an image of the electric fields present at the surface of the sample. Some of these EMM photographs are shown in Fig. 6 and the measured depletion widths as a function of bias are plotted in Fig. 7. The depletion width measured from the photograph at zero bias is approximately 20 to 30 μ. Scans with the light microprobe yielded about 10 to 15 μ. In view of these very wide surface depletion layers the cube root dependence of depletion width with voltage (Fig. 7) is probably not a very reliable indication of bulk effects.

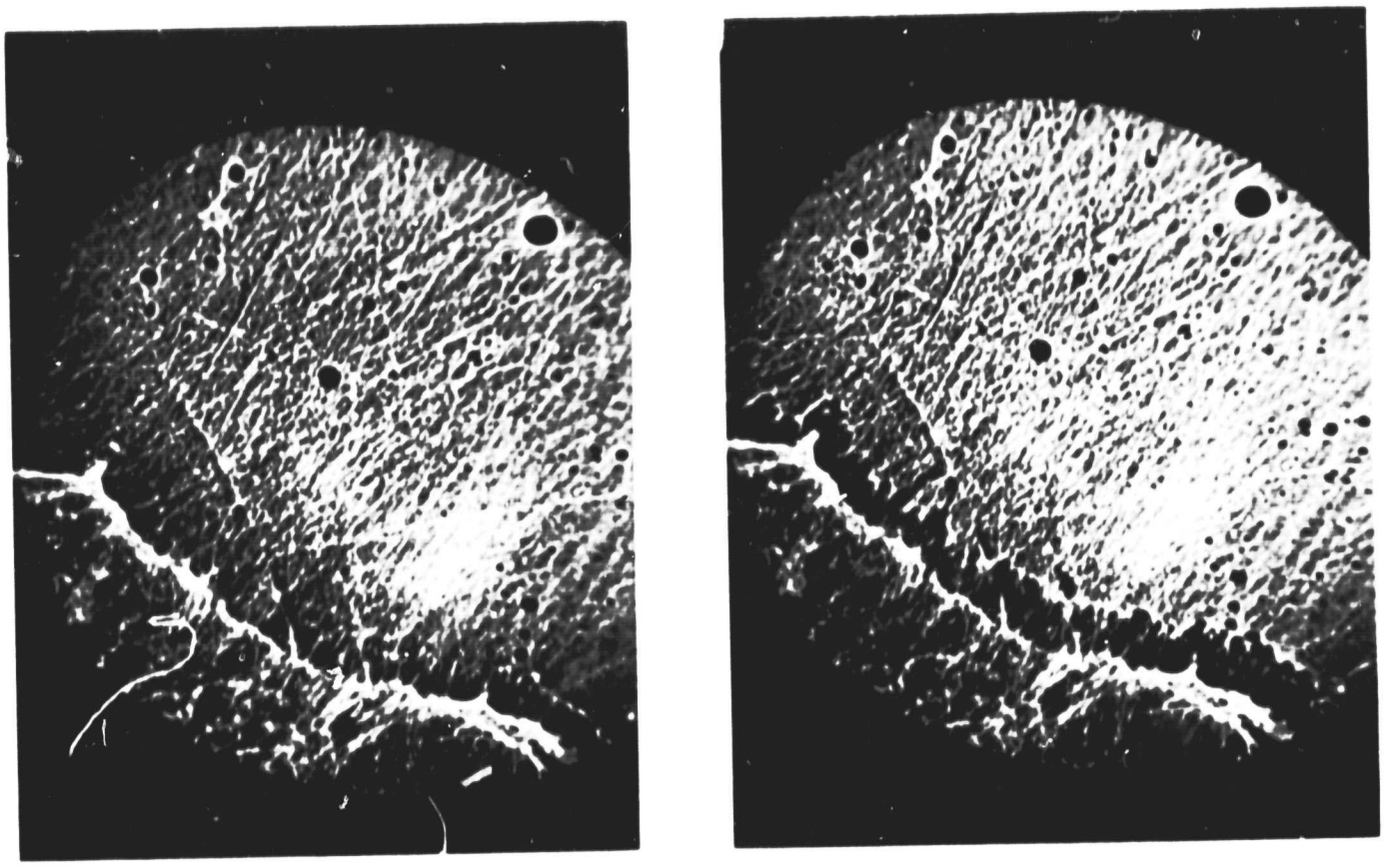

(a) V_{bias} = 0

(b) V_{bias} = -1 volt

(c) V_{bias} = -2 volts

(d) V_{bias} = -4 volts

Fig. 6. Electron mirror microscope photographs of a Cu_2S-CdS heterojunction under reverse bias. The Cu_2S side is in the lower left of the photographs. The depleted region is the dark band (Bevel angle is 90°, Magnification X150).

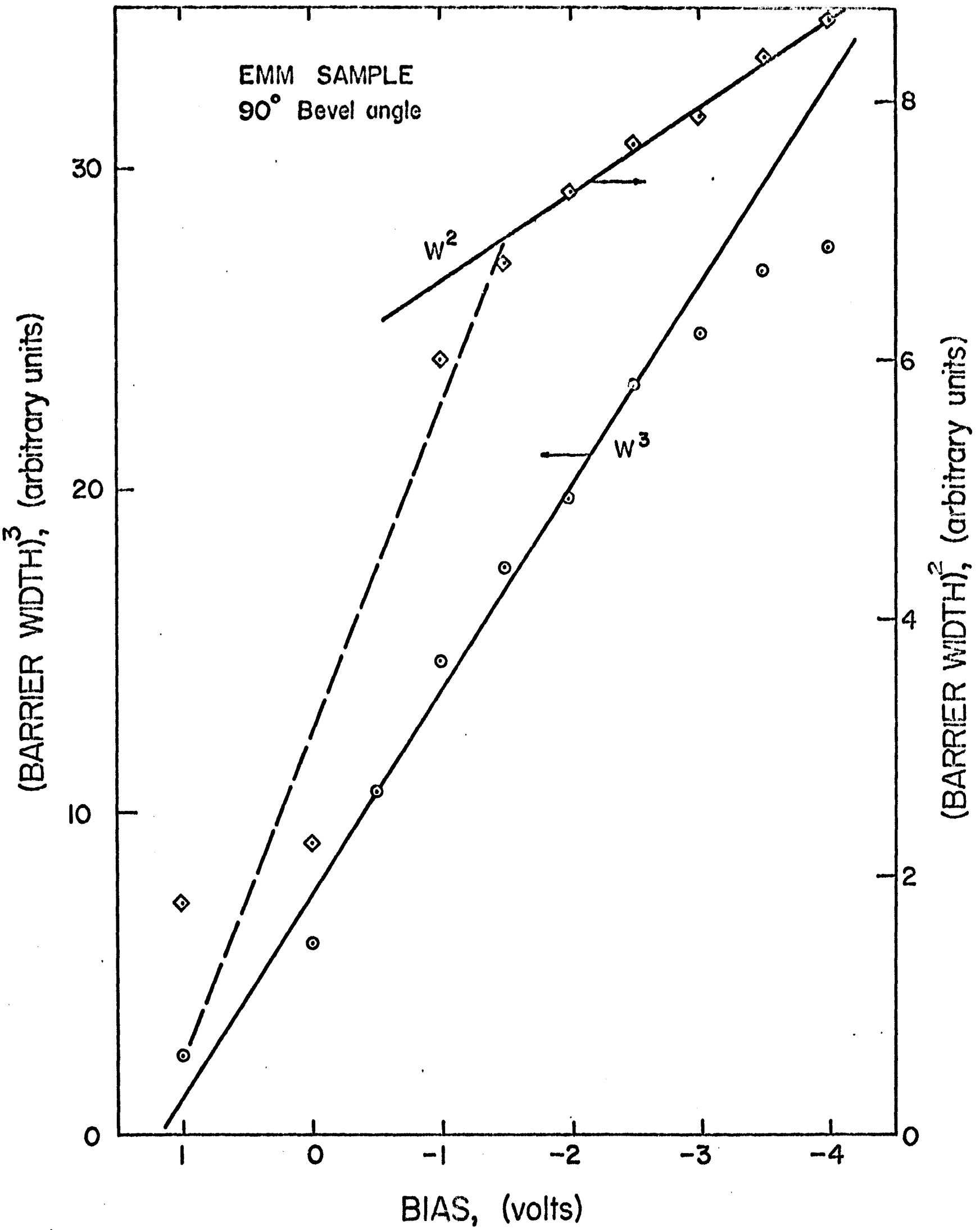

Fig. 7. Depletion width versus reverse bias voltage taken from electron mirror microscope results.

C. Effect of Chemical Etching

The other technique showing the wide depletion layers was discovered while using etches in an attempt to remove the damaged surface layer after bevelling. The use of concentrated H_2SO_4 + $KMnO_4$ as an optical quality etch for CdS has been reported.[3] Bevelled heterojunction samples immersed in this solution were found to etch on the CdS side except in a narrow band corresponding to the measured surface depletion width. A photograph of a sample etched in this way is shown in Fig. 8. The light probe response on the same sample is shown in Fig. 1 and corresponds with the width measured by the etching technique.

D. Cause of Wide Depletion Layers

The reason for the wide depletion layers at the surface is still in some doubt. Surface damage due to the bevelling operation and oxygen chemisorption are the obvious suspects. Desorption of oxygen by strong illumination in a nitrogen atmosphere was tried. Microprobe measurements made in the nitrogen atmosphere after attempted desorption were no different from those carried out in air. Heat treatment was found to eliminate the very wide depletion regions. For example, sample CdS(D3) which had a measured active region 100 μ wide (see Fig 10) when uncorrected for the 5° bevel angle showed a sharp decrease to about 5 μ after a 5 minute heat treatment at 250°C in air. It was thought that desorption of oxygen and annealing of surface damage might explain this reduction. The sample was then carefully rebevelled with removal of a 10 to 20 μ layer. Measurement of the active region showed it to be about 6 μ. Because the new surface damage did not result in widening of the surface depletion layer we conclude that heat treatment affected bulk properties near the junction in such a fashion as to inhibit formation of surface depletion regions. The narrow depletion widths measured with the light probe after heat treatment correspond to those measured capacitively and some widening of depletion regions with reverse bias is seen. However, because the light microprobe experiments are carried out under high-level injection conditions with consequent distortion of the depletion layer, they do not give a reliable measure of the voltage dependence of depletion width. Experiments will be carried out in the next few

Fig. 8. Photograph of the junction of CdS(E7) after etching in conc. H_2SO_4 + $KMnO_4$ solution for 2 minutes. The bevel angle was +5°. Cu_2S is at the top of the sample, the dark band is the unetched CdS depletion region, and the etched CdS is at the bottom (Magnification X100).

weeks using a 2μ by 2μ light spot instead of the present 2μ by 20μ line, and the light intensity will be reduced to the lowest possible level.

E. Capacitance vs. Bias Voltage

Capacitance versus reverse bias provides the most reliable measurements of depletion layer thickness, and probably of barrier height also. Fig. 9 shows $\frac{1}{C^2}$ versus applied bias for sample CdS(D3). The value of (N_D-N_A) obtained from the slope of this plot is in excellent agreement with the value obtained from the bulk resistivity of the crystal. Extrapolation of the curve in the forward direction yields a barrier height of 1.1 volts.

The insert in Fig. 9 shows the I-V characteristics for this sample in the dark and under illumination. The light characteristic is seen to remain below the dark characteristic over the entire plot, suggesting that leakage channels are not important in this sample. The barrier height obtained from the capacitance data on this sample is probably an accurate measure of the true barrier at Cu_2S-CdS heterojunctions. Several other samples, whose capacitance data indicate close to ideal Schottky barrier behavior, also have barrier heights of about 1 volt.

Capacitance data which do not follow $\frac{1}{C^2}$ vs.V behavior must be treated with great care. For example, positive curvature of the $\frac{1}{C^2}$ versus bias plot occurring near zero bias is indicative of a narrow intrinsic region, whereas calculation of doping profile from the slope would lead to the erroneous conclusion that the doping density was increasing as the metallurgical junction is approached. However, reliable capacitance data corrected for series and parallel resistance can in all cases yield a fairly accurate measure of depletion layer thickness. Interpretation of this width in terms of doping density and built-in voltage or barrier height is not always reliable.

III. SPECTRAL RESPONSE USING LIGHT MICROPROBE

The origin of the long wavelength response in Cu_2S-CdS heterojunctions and in Cu-CdS Schottky barrier cells has been a central problem of much of the past research. In the Cu_2S-CdS heterojunction case the magnitude of the response out to 1.0 micron and the good match of the response to the bandgap of Cu_2S leaves little doubt that the major portion of this response is due to photoemission from Cu_2S into the barrier region. However, following heat treatment many of our cells show marked decrease in the spectral response betwen 0.7 microns and 1.0 micron. The remaining long wavelength response between $E_{g_{CdS}}$ and 0.7 microns is characteristic

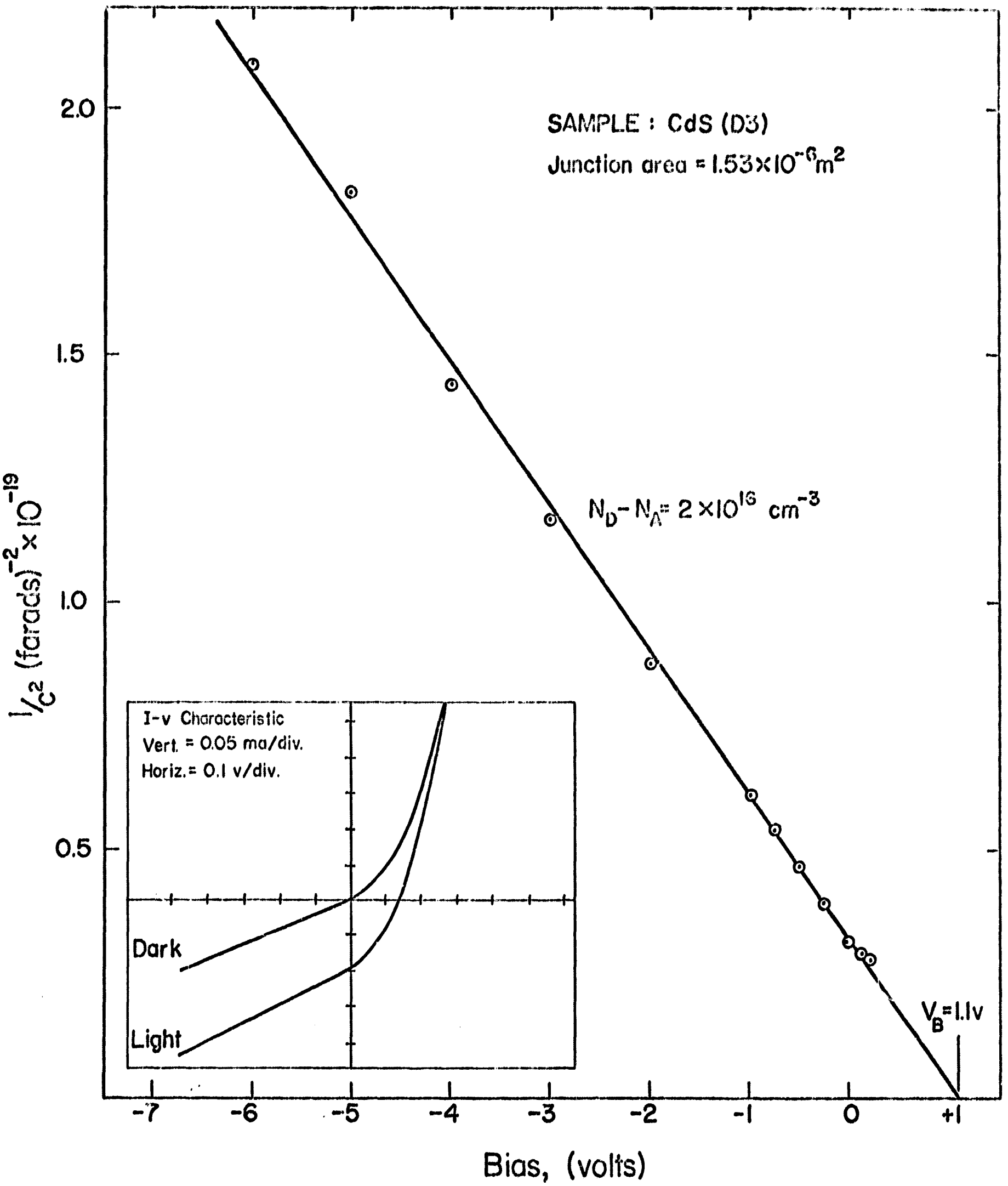

Fig. 9. $1/C^2$ versus reverse bias voltage for sample CdS(D3). Results indicate an ideal Schottky-type barrier with a built-in voltage V_B = 1.1 volts. The inset shows the dark and light I-V characteristics. Note that the forward current under illumination was below the dark current as expected for an ideal photodiode.

of heavily Cu doped CdS.[4] We have used the light probe to determine the spectral response as a function of position across a junction. The sample used had a wide surface depletion region which was helpful in making measurements to greater distances from the junction.

In Fig. 10 the results of several scans across the junction using short and long wavelength radiation are shown. The insets illustrate the sample geometry for the experiments. For the long wavelength experiments the light was focussed on the surface after passing through the CdS. This technique significantly reduces the amount of scattered light which can reach the large plane surface of the junction. The results show that significant red response is generated out to the same depletion widths delineated by the short wavelength experiments. Scattered red light which may reach the junction would not give rise to the step in the red response curves at the edge of the depletion regions. However, there is a possibility that the red response measured here is due to surface states and is not truly representative of the bulk response.

In Fig. 11 we show spectral response curves obtained on this sample at various distances from the junction. These curves show considerably more red response on the CdS side of the junction than in the Cu_2S side. Although the absorption of red light is much greater in the Cu_2S, the efficient carrier collection in the space charge region located on the CdS side is of great importance. It is possible that increased long wavelength efficiency would be realizable if the Cu_2S side of the junction were not degenerate. For a small loss in barrier height the extension of the space charge region a few tenths of a micron into the Cu_2S might lead to significant improvement in collection efficiency.

IV. EFFECT OF HEAT TREATMENTS

A. Short Heat Treatments

In order to study the effect of heat treatment on the heterojunctions, it was decided that samples should be prepared and all possible measurements be carried out, and that these samples should then be subjected to heat treatment and all measurements repeated. The measurements made on the samples included I - V characteristics in light and dark, capacitance versus reverse bias in light and dark, spectral response, and light microprobe scans with and without bias applied.

(1) Sample CdS (E) was prepared with a Cu_2S - CdS heterojunction on

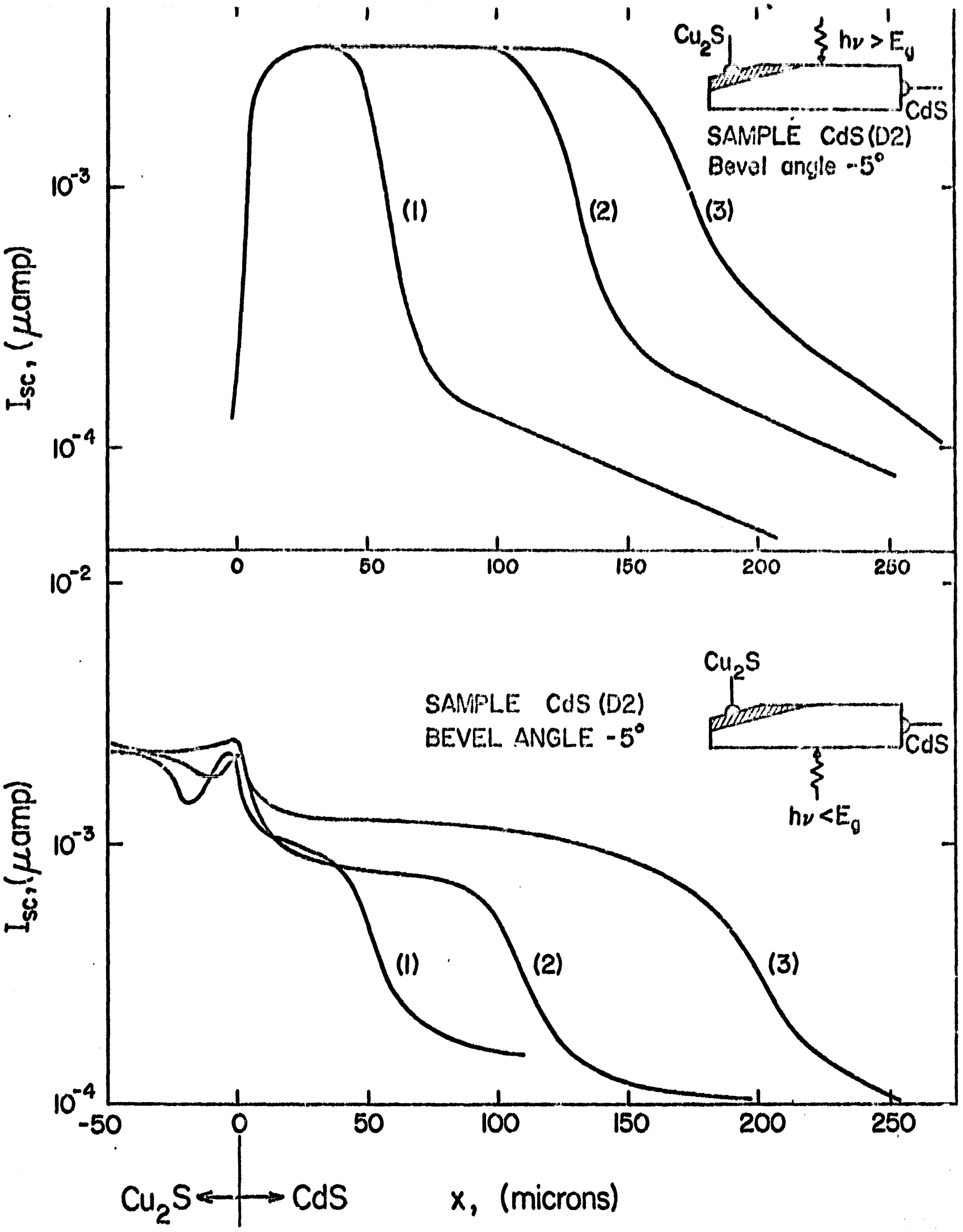

Fig. 10. Short-circuit photocurrent versus light spot position on sample CdS(D2). The top curves are for blue light incident on the frontwall side, and the bottom curves for red light incident on the backwall side. Numbers on the curves refer to three different positions along the bevelled junction. For -5° bevel angles, the measured distances should be multiplied by 0.087 to get the distance from the interface before bevelling.

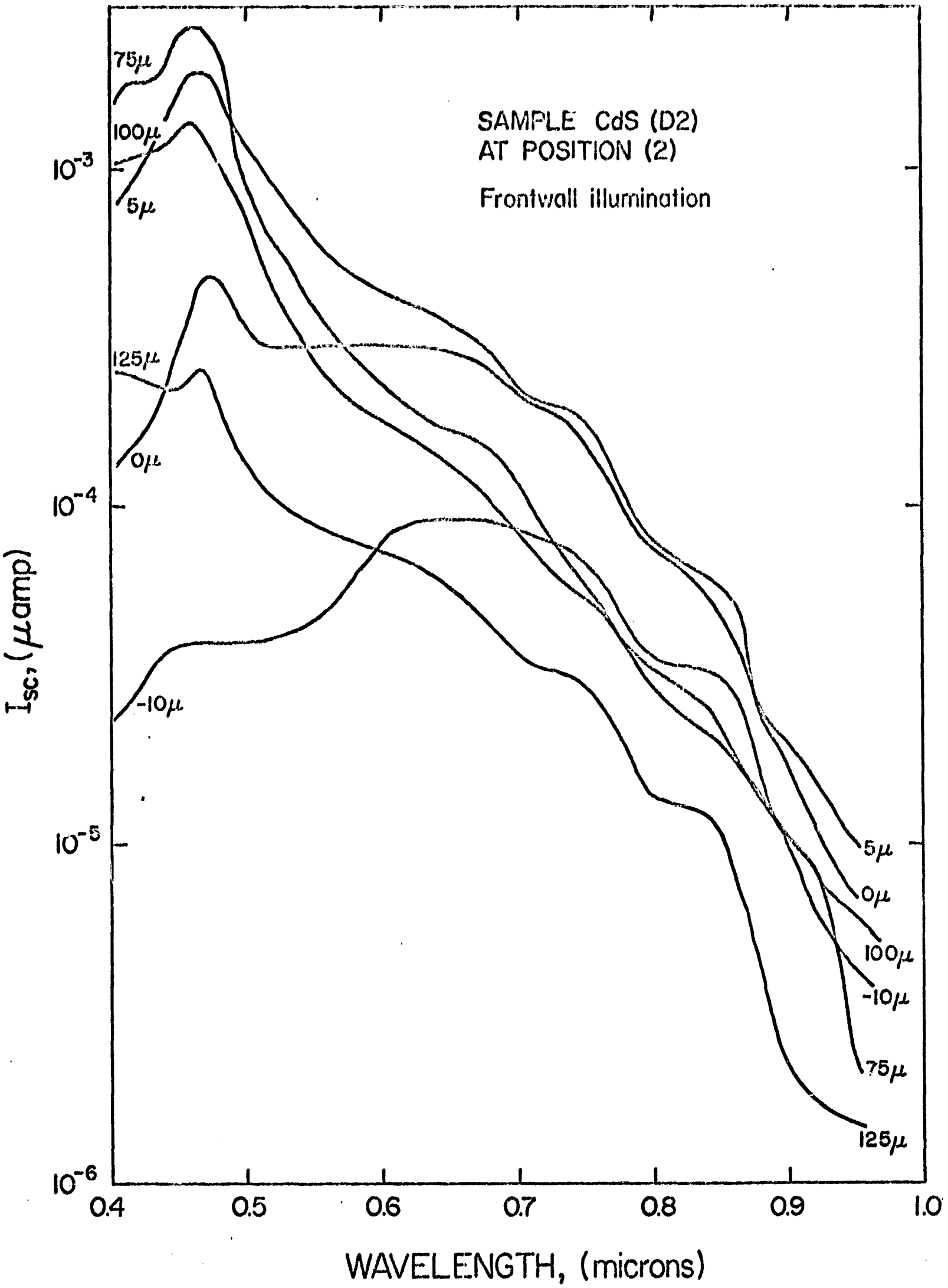

Fig.11. Spectral response curves at various distances from the junction of sample CdS(D^2). The numbers on the curves refer to distances from the interface along the bevelled surface. Positive distances are on the CdS side of the interface. These numbers should be multiplied by 0.087 to get the distance from the interface before bevelling.

one end of a CdS crystal and an electroplated Cu barrier cell on the other end. The Cu_2S layer was formed in a 15 minute dip at 74°C. After dipping, a thick gold layer was evaporated on the Cu_2S to form a good contact. On the other end of the crystal a thick layer of copper was deposited by electroplating from a cyanide solution. Both the Cu_2S and the Cu ends were bevelled at -5°. Capacitance data indicated fairly good Schottky barriers were formed on both ends with a slight indication of a narrow insulating region on the Cu_2S side. Surprisingly, the Cu side showed the best long wavelength response with an absorption edge at about 1μ. Representative I - V characteristics for the two ends taken before and after heat treatment are shown in Fig. 12. Comparison between the before and after heat treatment results are outlined in Table II. The heat treatment consisted of 2 minutes at 250°C in forming gas.

	Cu_2S Side		Cu Side	
	Before heat treat	After 2 min. at 250°C	Before heat treat	After 2 min. at 250°C
d (zero bias), μ	0.5	2	0.45	1
(N_d-N_a) cm^{-3}	1.05×10^{14}	1.1 to 4.5×10^{13}	$7.5 \times 9.6 \times 10^{13}$	1.1×10^{14}
R_p (zero bias), Ω	1.3K	22.5K	0.77 K	5.1 K
Longwave edge, A	6500	5300	9000	6500
I_{sc}, μ a	2.4	0.05	6	1.1
V_{oc}, volts	0.405	0.425	0.048	0.048
d (microprobe), μ	0.9	0.7	7.1	1.2

TABLE II. Properties of sample CdS(E) before and after heat treatment in a forming gas atmosphere.

(2) Sample CdS(E7) was a Cu_2S-CdS heterojunction formed by a 1 hour dip at 74°C. The sample was bevelled at +5° and then etched for 2 min.

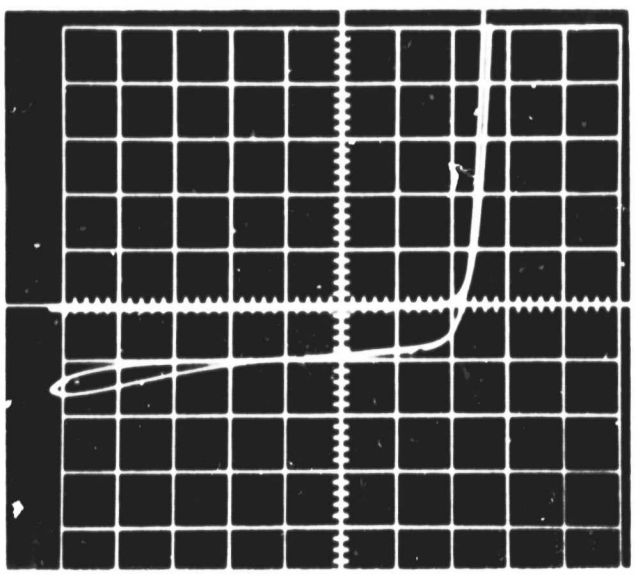

(a) Cu_2S side before heat treatment
Vert. = 0.01 ma/div
Horiz. = 0.2 v/div

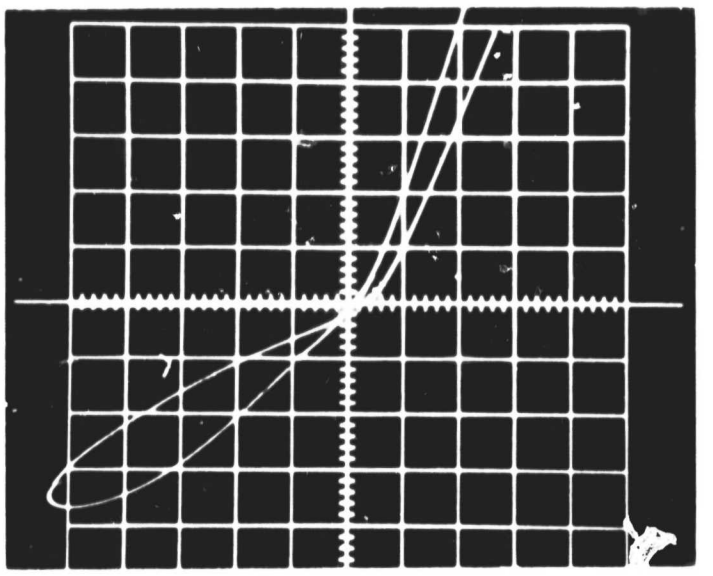

(b) Cu side before heat treatment
Vert. = 1.0 ma/div
Horiz. = 0.5 v/div

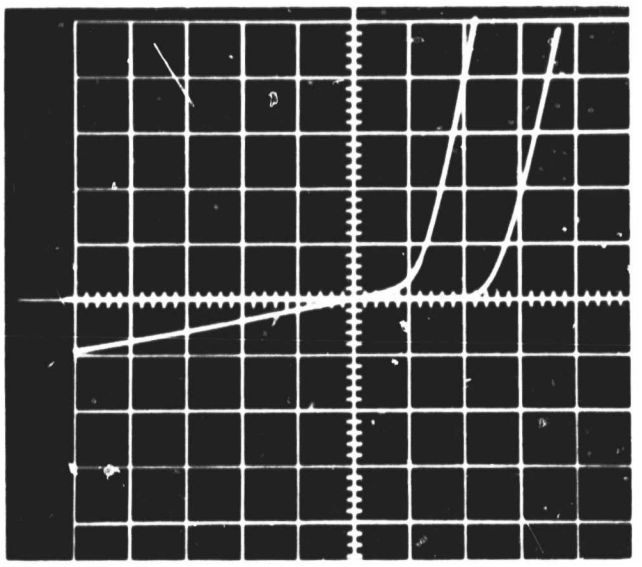

(c) Cu_2S side after heat treatment
Vert. = 1.0 ma/div
Horiz. = 0.5 v/div

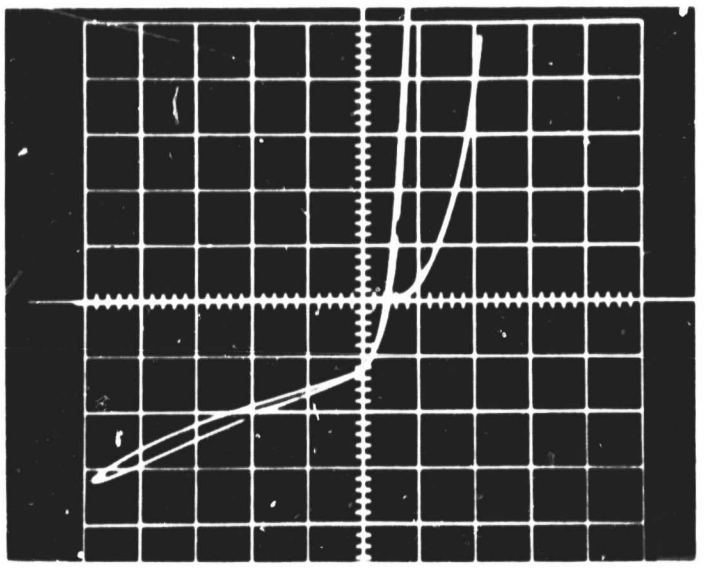

(d) Cu side after heat treatment
Vert. = 0.05 ma/div
Horiz. = 0.5 v/div

Fig. 12. I-V characteristics of sample CdS(E) before and after heat treatment for 2 minutes at 250° C in forming gas. The higher current curves are for strong backwall illumination with a tungsten source.

in concentrated H_2SO_4 + $KMnO_4$. Capacitance data resulted in a linear $1/C^2$ vs. V plot with $(N_D-N_A) = 1.3 \times 10^{15}$ cm^{-3}. Slight positive curvature near zero bias indicated a narrow insulating layer is present about 0.4 micron thick. This sample showed effects on V_{oc} which are typical of many of our non-heat-treated samples. Under bright white illumination from a tungsten lamp, $V_{oc} = 0.288$ volts and $I_{sc} = 2.35$ microamp. Inserting a Corning 2-64 filter in the light beam (passes wavelengths greater than 7000A) <u>increased</u> the measured open-circuit voltage to $V_{oc} = 0.315$ volts, and I_{sc} decreased to 0.82 microamp. This behavior can be attributed to increased leakage in the presence of bandgap light. The sample was then heat-treated for 30 seconds in air at 250°C. The capacitance data indicate a decreased net donor density to at least 5 microns from the junction with $(N_D-N_A) = 6.3 \times 10^{14}$ cm^{-3}. The data also indicate a widened insulating or intrinsic region about 1 micron in width. Repeating the measurements of V_{oc} and I_{sc}, we now found that without the 2-64 filter, $V_{oc} = 0.403$ volts and $I_{sc} = 4.2$ microamp, and with the filter, $V_{oc} = 0.396$ volts and $I_{sc} = 0.8$ microamp. The effect of the short heat treatment can be interpreted as a decrease in the leakage paths. The I-V characteristics for this sample are shown in Figure 13. It is interesting to compare the forward characteristics with those sketched in Figures 3 and 4 for the leakage model. Note that the effect of heat treatment is to increase V_B' and V_B''. Also V_{oc} is increased as would be expected for decreased leakage current. Note also that in the reverse direction, the current with light on is markedly decreased after the heat treatment. This reduction corresponds to a diminished gain effect under reverse bias.

The behavior of the I-V characteristics shown in Figs. 12 and 13 illustrates many of the features which are predicted by the generalized leakage-path model described previously.

B. <u>Effect of Extended Heat Treatment on the Spectral Response</u>

A single crystal cell (4-46) was fabricated from 1 ohm-cm CdS by dipping in an acidified CuCl solution for 2 hours at 90°C. After measuring the dark I-V characteristic and the backwall spectral response, the cell was sealed in an evacuated ampoule (P less than 10^{-5} torr) and heat treated for 1 hour at 300°C. The backwall spectral response was then remeasured. The results, before and after heat treatment, are presented in Fig. 14, normalized to a

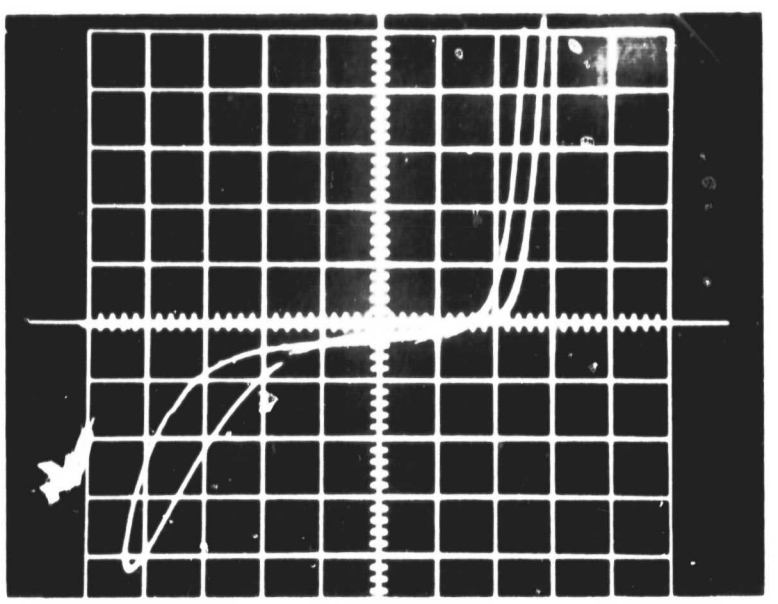

(a) Before heat treatment.
Vert. = 0.01 ma/div.
Horiz. = 0.2 v/div.

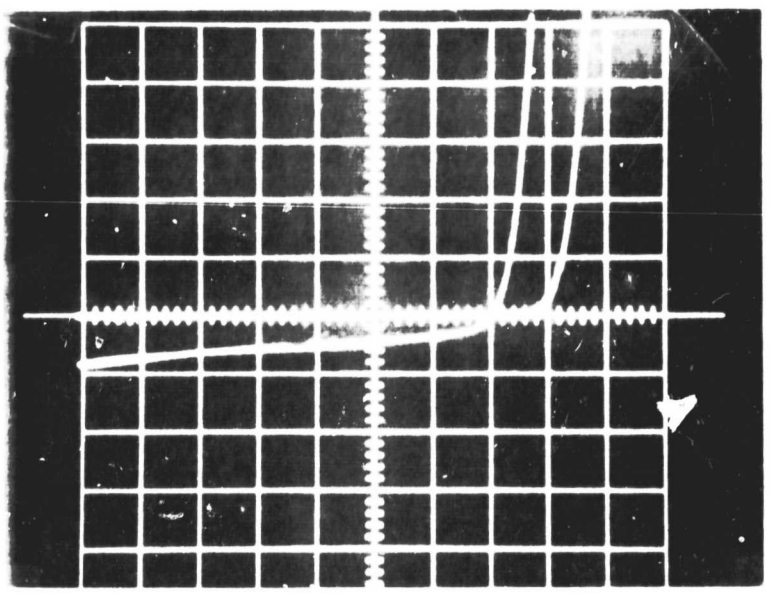

(b) After heat treatment.
Vert. = 0.01 ma/div.
Horiz. = 0.2 v/div.

Fig. 13. I-V characteristics of sample CdS(E7) before and after heat treatment for 30 seconds at 250° C in air. The higher current curves are for strong backwall illumination with a tungsten source.

photon flux of $5.8 \times 10^{14} cm^{-2} sec^{-1}$. The response beyond 700 m μ is down by two orders of mangitude as a result of the heat treatment, but at 550 m μ it has decreased only by one. The short circuit current in white tungsten light of 280 mw/cm^2 integrated power was decreased from 4.5 μ a to .053 μa by the heat treatment. The open circuit voltage of the cell after heat treatment was 450 mv in white light from a focused microscope illuminator, and increased to 490 mv when a 2-64 filter (which transmits for wavelengths greater than 700 m μ) was inserted.

The capacitance of this sample was also measured, before and after heat treatment. Before heat treatment, the measured capacitance in the dark increased with increasing reverse bias - a meaningless result. After heat treatment, only a very slight voltage dependence of capacitance in the dark was observed. With the sample exposed to the room light, the voltage dependence was more pronounced, and showed the unusual behavior indicated in Fig. 15. The decrease in capacitance for small forward and reverse bias is similar to the case of two diodes back to back, as obtained with "isotype" heterojunctions.[5]

The effect of the heat treatment can be qualitatively interpreted in the following way. On the basis of these and other data, the fairly good wavelength response (out to 1 μ) before heat treatment seems to be associated with an abrupt $Cu_{2-x}S$-CdS interface with an epitaxial relationship between the two structures, and thus may depend primarily on absorption in the $Cu_{2-x}S$. The spectral response for wavelengths only slightly longer than the CdS band edge, i.e., 530 - 600 mμ, may be due to a two-stage optical process via copper centers in the CdS.[6] In this case the $Cu_{2-x}S$ acts only as a contact and could be replaced by any other conductor. The extended heat treatment destroys the epitaxial relationship between $Cu_{2-x}S$ and the CdS, and thus makes the passage of electrons across the interface into the CdS more difficult. The absorption process in the CdS via copper centers still occurs, and the component of photocurrent due to this process depends on hole flow across the interface into the $Cu_{2-x}S$. It is presumed that this process is not affected so drastically by the "damaged" interface, so that the photoresponse near the CdS band edge is still high relative to that for longer wavelengths.

V. A STUDY OF CU_2S-CdS "MESA" DIODES

Sample #4-58 was prepared by dipping the "A" face of a CdS single crystal (50 ohm-cm) in CuCl at 90°C for 2 hours. The resistivity of the Cu_2S layer, measured by the four-point probe method, was.004 ohm-cm. Fig. 16 shows

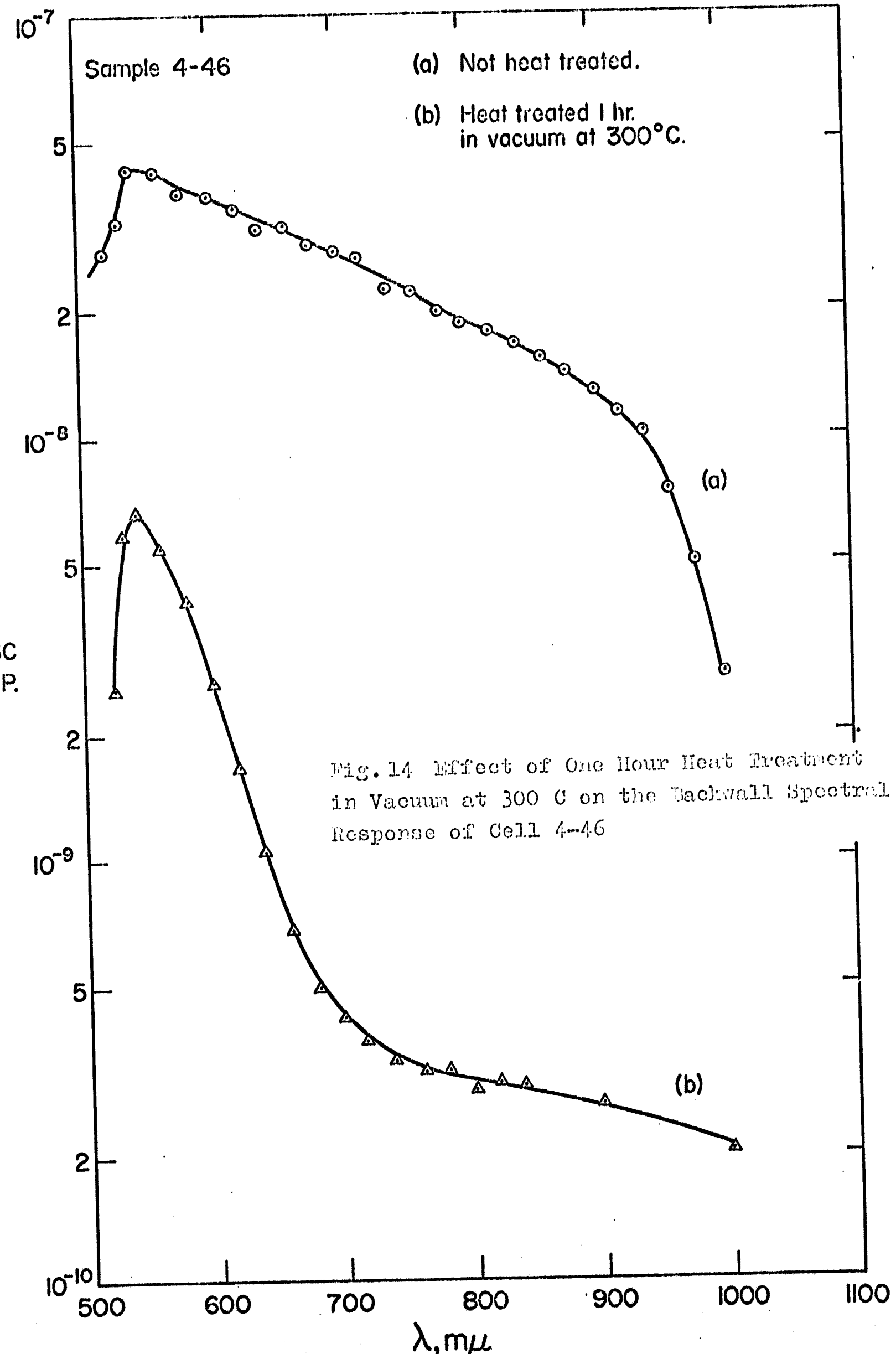

Fig. 14 Effect of One Hour Heat Treatment in Vacuum at 300 C on the Backwall Spectral Response of Cell 4-46

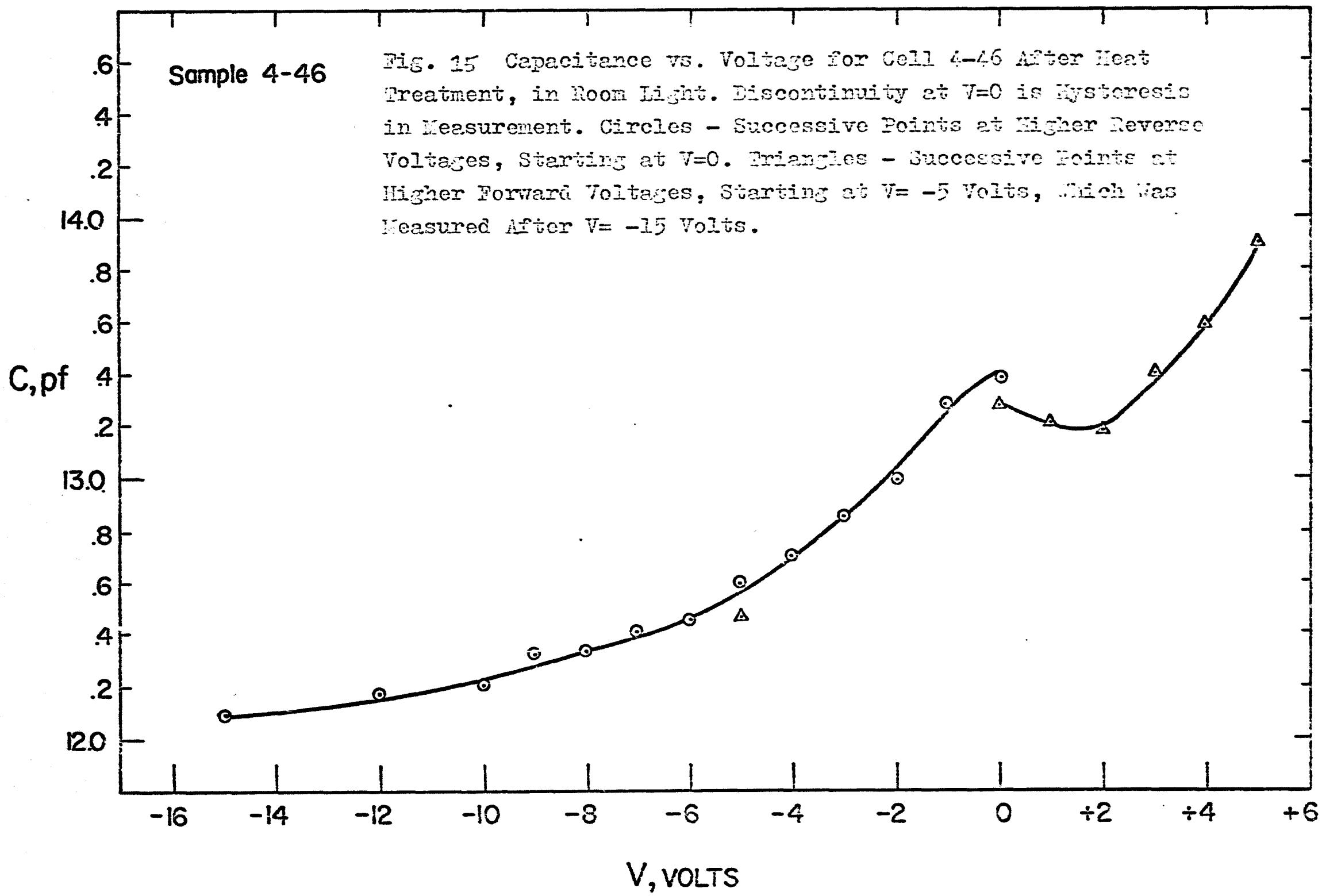

Fig. 15 Capacitance vs. Voltage for Cell 4-46 After Heat Treatment, in Room Light. Discontinuity at V=0 is Hysteresis in Measurement. Circles - Successive Points at Higher Reverse Voltages, Starting at V=0. Triangles - Successive Points at Higher Forward Voltages, Starting at V= -5 Volts, Which Was Measured After V= -15 Volts.

the backwall spectral response of the cell, normalized to a photon flux of 5.8×10^{14} $cm^{-2}sec^{-1}$.

A number of mesas were then etched on this sample, in the manner described in the Second Quarterly Progress Report. Capacitance-voltage curves (in the dark) for three of these mesa diodes are shown in Fig. 17. The measuring frequency was 1 MHz. In the figure, a "barrier voltage" of 0.8 volt has been assumed, which was in reasonable agreement with extrapolations of the forward I-V characteristics to zero current. The slopes on the log-log plot are seen to correspond more closely to the "linear graded" junction case than to the "abrupt" case, although it is possible that interfacial or trapping states are affecting the voltage dependence. The series resistance values in the figure, although quite high, did not necessitate a correction of the capacitance values, as discussed in the Second Quarterly Progress Report, p. 5, equation (7).[1]

Point-by-point I-V curves for two of these mesa diodes, in the dark, are presented in Figure 18. The numbers adjacent to the curves are the diode "A" factors. These large values of "A" cannot be interpreted in the absence of data on the temperature variation of the I-V curves. Such data will be acquired during the next report period.

Table III below summarizes the relevant data for these three diodes.

TABLE III. SUMMARY OF DATA FOR THREE "MESA" DIODES, CELL #4-58

MESA	R_s, ohms	A, cm^2	C(V=0)/A, pf/cm^2	G(V=0), mhos	J_o, amp/cm^2
1	2780	4.03×10^{-4}	5.33×10^{3}	2.11	
2	6110	3.41×10^{-4}	3.22×10^{3}	0.96	5.10×10^{-5}
3	2480	8.28×10^{-4}	4.50×10^{3}	7.11	4.2×10^{-4}

C(V=0) and G(V=0) are the 1 MHz capacitance and conductance, respectively, in the dark, at zero DC bias.

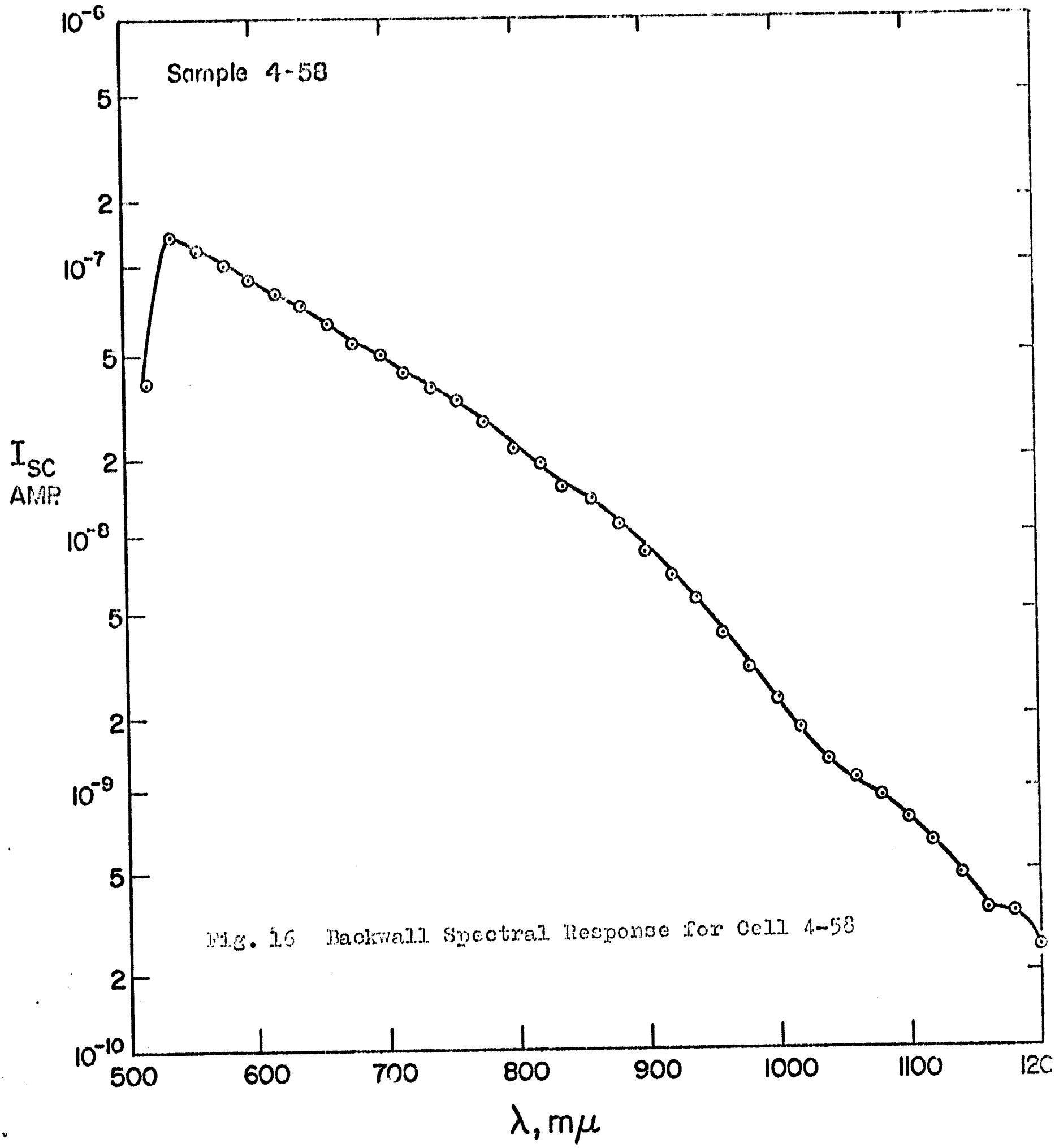

Fig. 16 Backwall Spectral Response for Cell 4-58

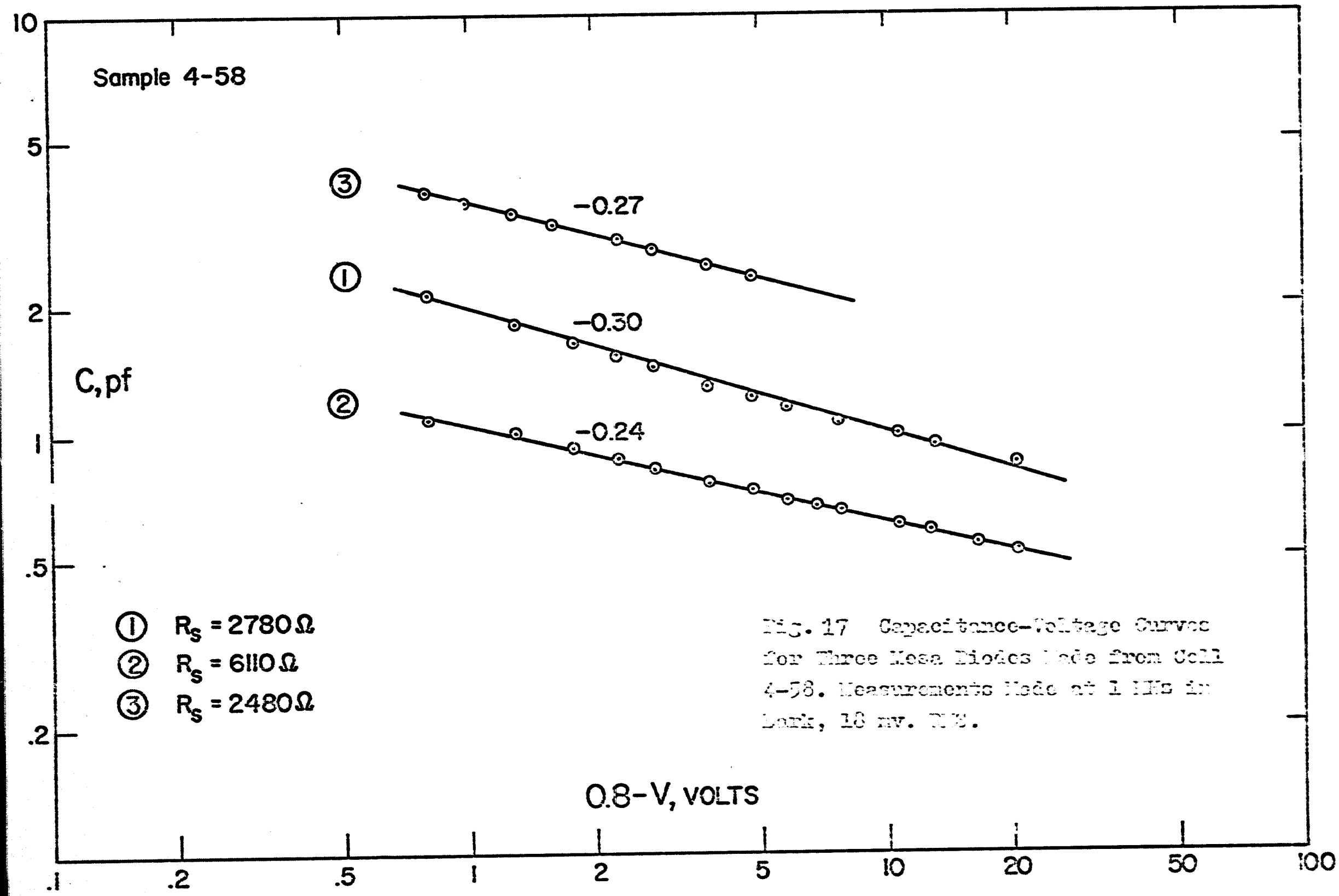

Fig. 17 Capacitance-Voltage Curves for Three Mesa Diodes Made from Cell 4-58. Measurements Made at 1 MHz in Dark, 18 mv. R.M.S.

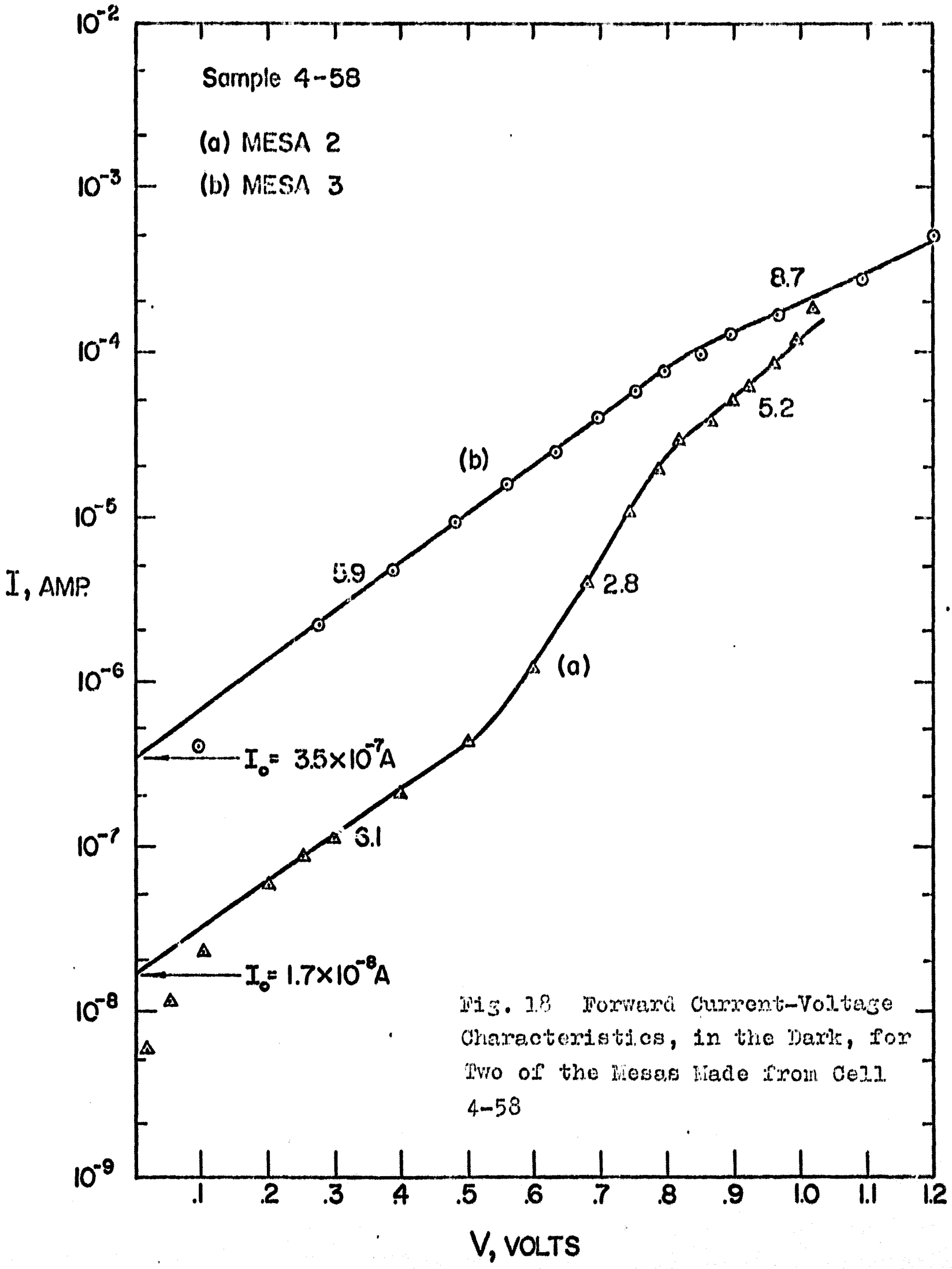

Fig. 18 Forward Current-Voltage Characteristics, in the Dark, for Two of the Mesas Made from Cell 4-58

VI. OUTLINE OF FUTURE WORK

1. Explore further the correlation between leakage paths and photoconductivity gain under reverse bias, in order to develop a specific model that will also be consistent with other measured properties of the photovoltaic cells.

2. Study the effect of short heat treatments on more Cu_2S-CdS and Cu-CdS junctions, using dark and light I-V characteristics, capacitance data, and light probe measurements.

3. Use a 2 micron by 2 micron light spot to scan parallel to the bevelled junctions and check if high gain regions correspond to low I_{sc} regions.

4. Measure the effect of light intensity on the gain. The gain should be greatly reduced when the injected carrier density is reduced.

5. Study the multiplication effect for wavelengths longer than the CdS band edge in greater detail, and attempt to correlate it with other cell parameters.

6. Systematically vary certain parameters of cell fabrication, such as crystallographic orientation of CdS, surface condition prior to dipping, addition of various salts to the dipping solution, and time in the dipping solution, and correlate with cell properties and performance.

7. Investigate effects of combinations of bias light and bias voltage on the cell output.

8. Obtain preliminary low-temperature data.

REFERENCES

1. R.H.Bube, W.D.Gill, and P.F.Lindquist, Report No. SU-DMS-68R-C4 (March 1968).
2. Measurements were made by Dr. F. English of Sandia Corporation, using the Litton Corporation's electron mirror microscope.
3. J.E.Rowe and R.A.Forman, J.Appl.Phys. 39, 1917 (1968)
4. R.H.Bube, E.L.Lind and A.B.Dreeben, Phys.Rev. 128, 532 (1962)
5. C. Van Opdorp and J.Vrakking, Solid State Electronics 10, 955 (1967)
6. R.E.Halsted, et al., Phys.Rev. Letters 2, 420 (1959)